DNA-Based Assembly of Metal Nanoparticles

Christof M. Niemeyer*[a] and Ulrich Simon*[b]

Keywords: DNA / Materials science / Nanoparticles / Self-Assembly / Supramolecular Chemistry

In this microreview we describe the principles of DNA-based assembly of metal nanoparticles in one, two and three dimensions. Different methods of liquid-phase synthesis of metal nanoparticles as well as their functionalisation with DNA are introduced. The concepts developed up to now for the assembly are explained, with selected examples to illustrate the properties of these assemblies as well as emerging applications.

1. Introduction

Modern chemical synthesis of metal nanoparticles is rooted in the famous experiments of Michael Faraday in the mid-nineteenth century, who showed that the reduction of tetrachloroaurate $[AuCl_4]^-$ with phosphorus as a reducing agent in aqueous solution leads to ruby-red solutions.[1] Today, we know that this reaction leads to the formation of gold nanoparticles in the size range between 3–30 nm,[2] and that the red colour results from the collective oscillation of surface electrons induced by the electric field of the entering light.[3] Since that time many different synthetic routes have been developed in order to obtain metal nanoparticles of different size and shape, all of which, in principle, follow the same strategy, i.e. the reduction of a metal salt in the presence of a stabilizing organic ligand. In the early 1990s these nanoparticles became a new chapter in chemistry. The development of high resolution physical measurements together with the elaboration of theoretical methods applicable to mesoscopic systems brought forth a lot of fascinating ideas about how these nanoparticles can provide new technological breakthroughs, for example in

[a] Universität Dortmund, Fachbereich Chemie, Biologisch-Chemische Mikrostrukturtechnik,
Otto-Hahn Str. 6, 44227 Dortmund
Fax: +49-231-755-7082
E-mail: christof.niemeyer@uni-dortmund.de
[b] Institut für Anorganische Chemie, RWTH Aachen,
Landoltweg 1, 52056 Aachen, Germany
Fax: +49-241-80-99003
E-mail: ulrich.simon@ac.rwth-aachen.de

Ulrich Simon was born in Essen in 1963. He studied chemistry at the University of Essen and obtained his diploma in 1990. In 1992 he obtained his doctorate (Dr. rer. nat.) in Essen and his habilitation in 1999. Since May 2000 he has held the Chair of Inorganic Chemistry and Electrochemistry at the RWTH Aachen University. The main interest of his current research includes the synthesis and electrical properties of metal and semiconductor nanoparticles and of nanoporous materials as well as their application in molecular electronics and chemical sensing.

Christof M. Niemeyer is Professor of Chemistry at the University of Dortmund (Germany) where he holds the chair of Biological and Chemical Microstructuring. He was born in Cloppenburg and studied chemistry at the University of Marburg. His PhD thesis on the development of organometallic receptor molecules at the Max-Planck-Institut für Kohlenforschung in Mülheim/Ruhr under the supervision of Manfred T. Reetz was followed by a postdoctoral fellowship at the Center for Advanced Biotechnology in Boston (USA) with Charles R. Cantor, where he switched research fields to study biomolecular recognition systems. He went back to Germany, where he received his habilitation at the University of Bremen before moving to Dortmund in 2002. He is interested in semisynthetic DNA-protein and nanoparticle-conjugates and their applications in life-sciences, catalysis and molecular nanotechnology.

MICROREVIEWS: This feature introduces the readers to the authors' research through a concise overview of the selected topic. Reference to important work from others in the field is included.

nanoelectronic, diagnostic or sensing devices.[4–10] Basic research has disclosed that nanoparticles exhibit many properties that are somehow between that of a macroscopic solid or bulk material and that of a single atom or molecule.

Nanoparticles with a diameter of between one and several tens of nanometres, which fall in the intermediate size range between molecules and macroscopic solids, exhibit an electronic structure that is somewhere in between the discrete electronic levels of an atom or molecule and the band structure of a bulk material.[11] Although the concept of band structure can still be applied below a certain size these nanoparticles show a size-dependent splitting of the energy levels that replaces the continuum of the energy bands. In this intermediate state matter reveals new physical properties which now depend on the size of the object under consideration. As its origin is in the quantisation of electronic states, this size-dependent change of physical properties is called the *quantum size effect* (QSE) or *size quantisation effect*.

This raises fundamental questions about the design of "artificial molecules" or "artificial solids" built up from nanoscale subunits that finally lead to a new state of matter. This requires the ordered assembly of uniform nanoparticles in one, two or three dimension, leading finally to the formation of an artificial solid or super lattice. Such an array of nanoparticles exhibits delocalised electron states that depend on the strength of the electronic coupling between the adjacent nanoparticles, whereas the electronic coupling depends on the particle size, the nature and the covering density of the stabilizing organic ligands, on the particle spacing, and on the packing symmetry.[11]

Thus it is a great challenge to organize nanoparticles in one to three dimensions in order to study the electronic and optical coupling between the particles, and to even utilize these coupling effects for the set-up of novel nanoelectronic, diagnostic or nanomechanical devices.[9]

Several attempts have been made to assemble metal nanoparticles in one to three dimensions. These range from Langmuir–Blodgett techniques,[12] molecular self-assembly[13] via covalent linkage[14] and electrostatic coupling up to the deposition within or at pre-structured surfaces.[15] However, most of these methods suffer from a lack of recognition and binding specificity.

In contrast, biomolecules, such as proteins and nucleic acids, have almost perfect binding properties and biochemical functionality that have been optimised over billions of years of evolution. Since they are more readily available by synthetic chemical means and are more convenient to handle than proteins, nucleic acids have preferentially been used for the functionalisation of nanoparticles to provide highly specific binding sites.[16,17] Proteins have also been employed to extend the binding capabilities of inorganic nanoparticles, however, instead of simply utilizing their binding properties, a great challenge is the combination of the intrinsic functionality of many proteins, for instance, optic, catalytic, mechanic or switching capabilities, with the distinct properties of nanoparticles.[18] This topic, however, is beyond the scope of this review article, and we will instead focus here on DNA as a construction material in nanosciences.

The enormous specificity of Watson–Crick base-pairing allows the convenient programming of artificial DNA receptor moieties. The power of DNA as a molecular tool is enhanced by our ability to synthesise virtually any DNA sequence by automated methods[19] and to amplify any DNA sequence from microscopic to macroscopic quantities by the polymerase chain reaction (PCR).[20] Another very attractive feature of DNA is the great mechanical rigidity of short double helices, such that they behave effectively like a rigid rod spacer between two tethered functional molecular components on both ends up to approximately 100 nm. Moreover, DNA displays a relatively high physicochemical stability, and Nature provides us with a variety of highly specific enzymes that allow the processing of the DNA material with atomic precision and accuracy on the angstrom level. No other (polymeric) material offers these advantages, which are ideal for molecular construction in the range from about 5 nm up to the micrometer scale. Consequently, DNA has already been used extensively for construction on the nanometre scale,[21] and recent advances indicate its applicability for fabricating nanomechanical devices.[22,23] Hence, DNA holds the promise of allowing the bottom-up self-assembly of complex nanodevices, where, for example, in the course of further miniaturisation, conductive DNA-based structures could reduce time and cost in future nanofabrication.[24]

It is the aim of this microreview to acquaint the reader with the principle of DNA-based assembly of metal nanoparticles. Therefore, the second section introduces the different methods of liquid-phase synthesis of metal nanoparticles and their functionalisation with DNA. The third section will give an overview of the assembly of nanoparticles in one, two and three dimensions. The properties and the emerging applications of these assemblies will be discussed and illustrated with selected examples.

2. Materials Synthesis

2.1. Liquid-Phase Synthesis of Metal Nanoparticles

The synthesis of ligand-stabilized nanoparticles is usually based on the classical routes of colloid or organometallic chemistry. These are suitable for various metals, usually transition metals, as well as for many semiconductors which have technological applications in the bulk state.[7] Besides radiolytic[25] or photochemical[26] techniques and the controlled deposition of metastable organometallic compounds,[27–29] the most common ways of preparation are the chemical reduction of soluble metal salts by suitable reducing agents (e.g., hydrogen, boron hydride, methanol, citric acid, and others), and electrochemical reduction. In order to stabilize the nanoparticles, to control their size and shape and to prevent them from aggregating, organic ligands need to be added. These ligands are typical colloid chemical stabilizers or electron-donor ligands, like amines, phosphanes or thiols, which stabilize the particles electrostatically or ste-

rically. While the electrostatic stabilisation involves the coulombic repulsion between the particles caused by the charged surface of the nanoparticles and/or by the charge introduced by the respective ligand, steric stabilisation is achieved by ligand molecules that surround the particles as a protective shield. If DNA is used as a ligand, the negative charge of the ribose phosphate backbone introduces negative charge and leads to a predominantly electrostatic stabilisation of the nanoparticles.

The size of the particles is determined by the relative rates of nucleation and particle growth. However, the many control parameters affecting the particle size cannot be analysed separately, so that an established synthesis leading to a well-defined size for one particular metal cannot automatically be transferred to another metal. Nevertheless, many different liquid-phase synthetic routes have been developed which lead to distinct sizes with a narrow particle-size distribution, and which allow the preparation even in multigram scale.

For a detailed description of the synthesis and surface modification of metal nanoparticles the reader might be guided by Daniel and Astruc,[30] Bradley and Schmid,[7] and by Richards and Boennemann.[31] The following chapters will give a brief summary of synthetic routes in the liquid phase, with an emphasis on noble metal nanoparticles, that are typically applied for assembly processes in order to study size and coupling effects.

2.1.1. Chemical Reduction of Metal Salts

The salt reduction route with different types of stabilizing ligands and the wide range of chemical reduction agents has led to a huge variety of metal nanoparticles of different sizes and shapes, with the so-called Schmid cluster $[Au_{55}(PPh_3)_{12}Cl_6]$ being one of the most prominent examples.[32,33] Other examples are $[Pt_{309}phen^*_{36}O_{30}]$[33] or $[Pd_{561}phen_{36}O_{200}]$ (phen* = bathophenanthroline and phen = 1,10-phenanthroline).[34,35] These particles show an extremely narrow particle-size distribution and the idealised formulae of these compounds refer to the so-called geometric magic numbers. According to this model, the metal atoms tend to form a closed geometry of densest sphere packing, where one central atom is surrounded by a closed shell of 12 atoms as next neighbours and a second shell of 42 atoms surrounds this 13-atom arrangement to give a total of 55 atoms, and so on. Larger ligand-stabilized metal nanoparticles are typically not described by their atom number but by their mean diameter, whereas the size distribution typically increases with increasing particle size.

Another approach for the synthesis of nanoparticles involves block copolymers, which are able to form micelles upon addition of a polar or non-polar solvent. These micelles can be regarded as "nanoscopic reactors". After formation of the micelles in a non-polar solvent and addition of a soluble metal salt, the metal ions migrate into the hydrophilic core of the micelles where they are reduced to the metal by addition of a reducing agent. Consequently, the size of the nanoparticles depends on the size of the micelle as well as on the number of metal ions that have been provided to the micelle's core.

As most impressively demonstrated by Möller and coworkers, Au nanoparticles in polystyrene block polyethylene oxide (PS-b-PEO) hexagonally assembled micelles with rather regularly arranged particles 2.5, 4 or 6 nm in diameter can be obtained.[36,37] There, the association of PS-b-PEO for the formation of micelles in a non-polar solvent like toluene was utilized. After adding $LiAuCl_4$ to this solution, the salt was slowly dissolved as the Li^+ ions formed a complex with the polyethylene oxide. Thus, the $AuCl_4$ anions were incorporated as counterions into the micelles, where the nanoparticles were formed by reduction.

2.1.2. Electrochemical Composition of Metal Nanoparticles

An electrochemical route for the synthesis of nanoparticles from Pd or Ni and even from superparamagnetic Co has been developed by Reetz and co-workers.[38] This process, in which the particle size can be controlled in a simple manner by adjustment of the current density, makes use of a simple two-electrode setup in which the sacrificial anode consists of the bulk metal to be transformed into nanoparticles. The supporting electrolyte contains tetraalkylammonium salts, which act as stabilizing ligands in the abovementioned way. Thus, in the overall process the bulk metal is oxidized at the anode, the metal cations migrate to the cathode, and a consecutive reduction takes place with the formation of the ligand-stabilized nanoparticles. Particle sizes in the range of 1.4–4.8 nm and above with a narrow size-distribution can be obtained using this technique. The most striking advantage seems to be the broad variation of the corresponding ligand shell. Since the tetraalkylammonium ions are simply added to the reaction mixture, the thickness of the ligand shell can easily be varied by changing the length of the alkyl chain.

2.2. Synthesis of DNA-Functionalized Nanoparticles

The solid-phase synthesis of DNA oligomers as well as of other native and non-natural nucleic acid derivatives is nowadays routine technology, and DNA sequences up to about 120 nucleotides in length, modified with a large variety of chemical substituents, such as amino and thiol groups attached to the 3′- or 5′-terminus, are readily available by a multitude of commercial suppliers at relatively low costs. These materials are typically used in the synthesis of DNA-modified gold nanoparticles (DNA AuNPs). Most protocols for the synthesis of DNA AuNPs go back to the initial description of these materials by Mirkin and coworkers.[39] Briefly, citrate-stabilized AuNPs are simply mixed with DNA oligomers derivatized with alkylthiol groups at the 3′- or 5′-terminus, incubated for prolonged times of up to several days, and then purified by repeated centrifugation to remove unbound oligomers from the supernatant. The resulting DNA AuNPs are water-soluble and stable for months. Slight variations of the initial protocol have been reported by Mirkin[40] and Niemeyer.[41] The latter, for instance, has reported the synthesis of "oligofunc-

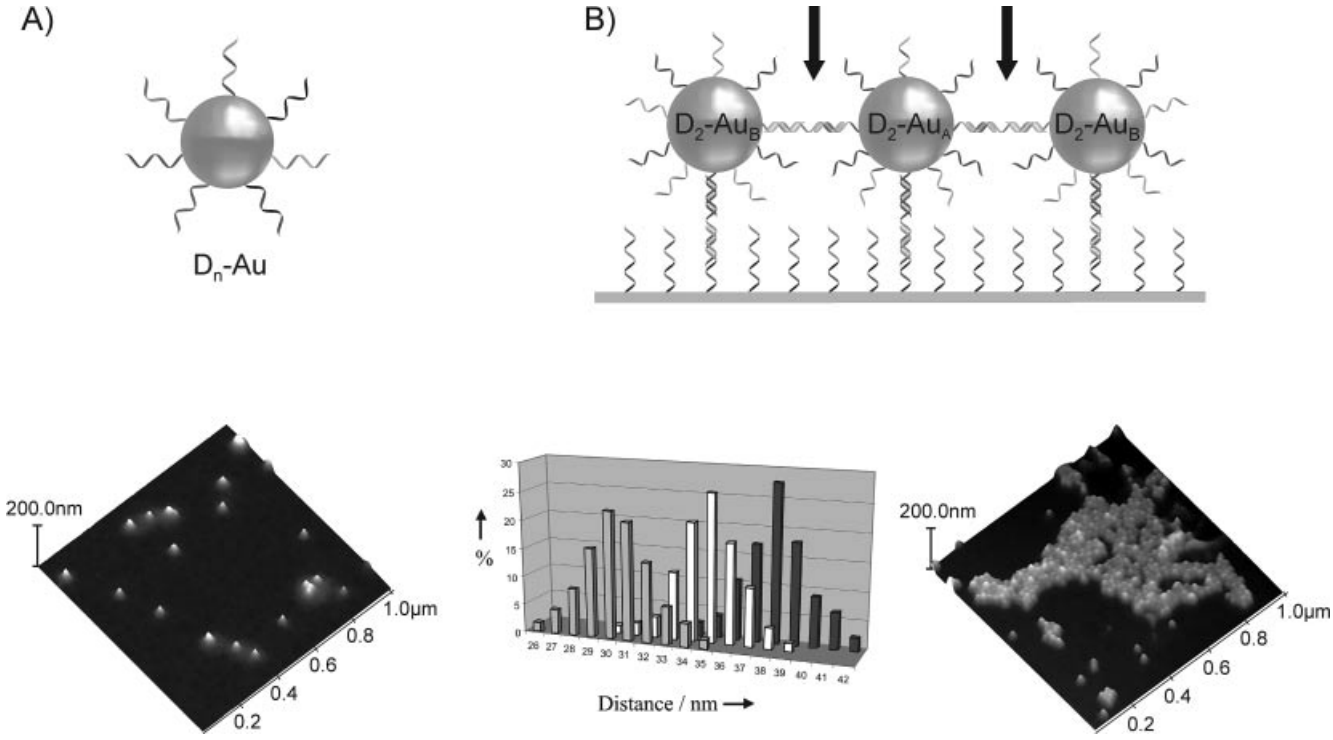

Figure 1. A) Schematic drawing of oligofunctional DNA–gold nanoparticle conjugates (**D_n-Au**) containing various coding oligonucleotides. B) Schematic drawing of DNA-directed immobilisation of cross-linked bifunctional DNA–gold nanoparticles (**D_2-Au**). Two different types of particles (**D_2-Au_A** and **D_2-Au_B**) are immobilized at surface-bound capture oligomers using one of the coding oligonucleotides and are simultaneously cross-linked using the second coding oligonucleotide. Note that both the immobilisation and the interparticle crosslinking is conducted by a trimolecular oligonucleotide linkage. Bottom: AFM images of layer assemblies prepared in the absence (left) or in the presence (right) of crosslinking oligonucleotide.[92] The inset shows the dependency of the particle's centre-to-centre distances on the length of the crosslinking oligomer used.[93]

tional" DNA AuNPs, that contain more than one coding sequence (**D_n-Au** in Figure 1).[42] The index *n* in **D_n-Au** denotes the number of different sequences attached to the nanoparticle, ranging from two (difunctional) up to seven (heptafunctional). The **D_n-Au** nanoparticles reveal almost unaltered hybridisation capabilities as compared to conventional monofunctional conjugates. Due to the extraordinary specificity of Watson–Crick base-pairing, the various oligonucleotide sequences can therefore be individually and selectively addressed as members of an orthogonal coupling system present at the particle's surface.

Applications of such oligofunctional DNA AuNPs are discussed below in Section 3.2.2. It is particularly noteworthy that it is most helpful for many applications to be able to quantify the coverage of the DNA AuNP's surface with DNA oligomers. To achieve this, the fluorescence-based assay of Demers et al.[43] is highly recommended. Moreover, DNA AuNP might, if necessary, be purified by gel electrophoresis, as described by Alivisatos and co-workers.[44,45]

Other approaches have been reported to increase the stability of DNA AuNPs, including the use of polymers[46] and dithiol[47] and trithiol linkers[48] between the DNA moiety and the gold particle. Interestingly, Brust and co-workers have used short peptides with the sequence CALNN to produce very stable AuNPs[49] that can also be further functionalised by attachment of DNA oligomers.

3. Nanoparticle Assemblies & Properties

3.1. Three-Dimensional Assemblies

3.1.1. DNA-Directed Self-Assembly

Following the initial approach of Mirkin's group, DNA hybridisation has been used to generate repetitive, three-dimensionally linked nanoparticle assemblies (Figure 2) where two non-complementary oligonucleotides are coupled in separate reactions with 13-nm gold particles by thiol adsorption.[39] A DNA duplex molecule containing a double-stranded region and two cohesive single-stranded ends, which are complementary to the particle-bound DNA, was used as a linker. Addition of the linker to a mixture of the two oligonucleotide-modified nanoparticles led to the aggregation and slow precipitation of the macroscopic DNA–nanoparticle network. This process is reversible. Since the nanoparticles contain multiple DNA molecules, the oligomerised aggregates are three-dimensionally linked, as can be seen by TEM. Typical images reveal close-packed assemblies of the colloids with uniform particle separations of about 6 nm, corresponding to the length of the DNA linker duplex.

This assembly scheme can also be used for the generation of binary networks comprised of different types of particles. Due to the specificity of Watson–Crick base-pairing, only heterodimeric "A-B" composites of alternating particles are

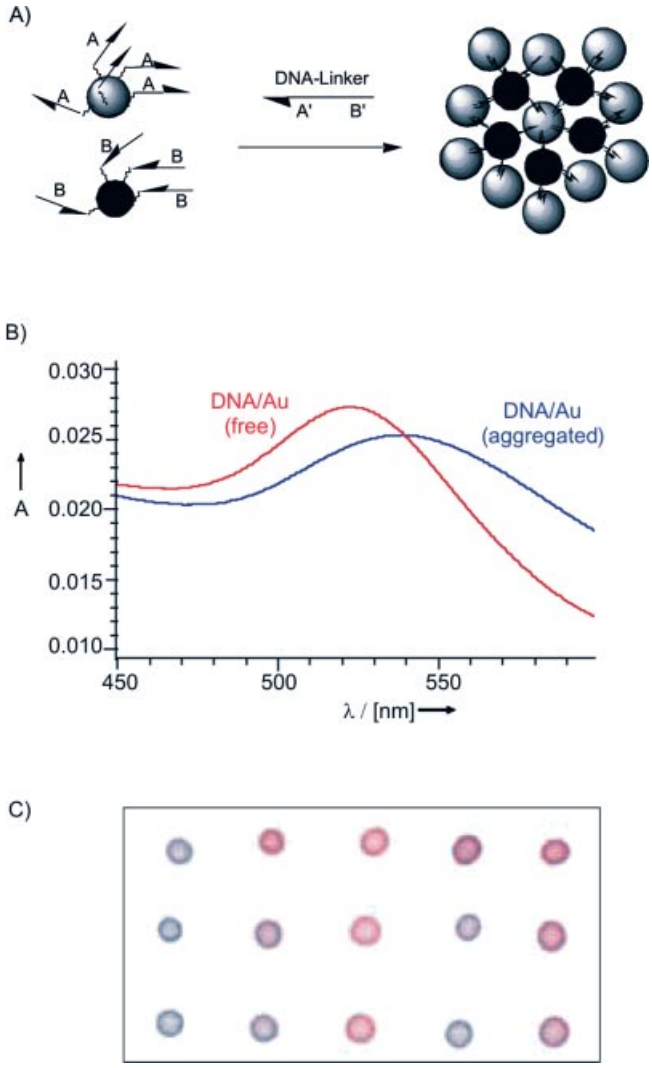

Figure 2. A) Three-dimensional assembly of gold colloids using DNA hybridisation. Two batches of gold particles are derivatized with non-complementary oligonucleotides by either 5′- or 3′-thiol groups. The nanoparticles are oligomerised with a single-stranded nucleic acid linker molecule. Note that only heterodimeric "A–B" linkages are present within the network. B) The network formation leads to a characteristic change in the plasmon absorption. The colour change can be used to macroscopically detect DNA hybridisation using an assay in which DNA/Au conjugates and a sample with potential target DNA is spotted on a hydrophobic membrane. C) Red spots indicate the absence of fully matched DNA, while blue spots are indicative of the presence of complementary target DNA. Data in part C) are reprinted from J.J. Storhoff et al. *Chem. Rev.* **1999**, *99*, 1849–1862. Copyright 1999, American Chemical Society.

formed (Figure 2). For example, two types of gold clusters of either 40 nm or 5 nm diameter have been assembled by DNA hybridisation. In the case of an excess of one particle, satellite-like aggregate structures can be generated and characterised by TEM. Similarly, it has been shown that oligonucleotide-functionalised CdSe/ZnS QDs can be specifically assembled with gold nanoparticles to form binary nanoparticle networks.[50] TEM analysis revealed that the hybrid metal/semiconductor assemblies exhibited the expected A-B structure, and fluorescence and electronic absorption spectroscopy indicated cooperative optical and electronic phenomena within the network materials.

Mirkin et al. have demonstrated that the oligomerisation of DNA-coated gold nanoparticles, depicted in Figure 2, can also be mediated by conjugates comprised of oligonucleotides attached to the streptavidin (STV) protein. Interestingly, the thermodynamically most stable oligomeric networks were only formed upon heating of the kinetically controlled adducts produced initially.[51] Additional topics of fundamental research on DNA/protein nanoparticle interaction concern the investigation of whether and how DNA-functionalised particles can be manipulated by DNA-modifying enzymes.[18] Particles of different morphology, especially rods and sticks, have also been assembled by means of DNA hybridisation.[52,53]

3.1.2. Materials Properties

Studies of DNA-linked gold nanoparticle assemblies concern the influence of the DNA spacer length on the optical,[54] electrical[55] and melting properties[56] of these networks. These experiments provided evidence that the linker length controls the size of the aggregates kinetically, and that the optical properties of the nanoparticle assemblies are governed by aggregate size.[54] In contrast, it has been found that the electrical properties of dry nanoparticle aggregates are not influenced by the linker length.[55] Although SAXS clearly indicates the linker length-dependent distances between particles in solution, the networks collapse upon drying to form bulk materials comprised of nanoparticles covered with an insulating film of DNA. These materials show semiconductor properties that are not influenced by the linker lengths.[55] The strongly cooperative melting effect of the nanoparticle networks[56] results from two key factors: the presence of multiple DNA linkers between each pair of nanoparticles, and a decrease in the melting temperature as DNA strands melt due to a concomitant reduction in local salt concentration. This mechanism, originating from short-range duplex-to-duplex interactions, is independent of DNA base sequences and should be universal for any type of nanostructured probe that is heavily functionalised with oligonucleotides.[56]

3.1.3. Applications

Gold nanoparticles functionalised with proteins have long been used as tools in biosciences.[57] For instance, antibody molecules adsorbed to 10–40-nm colloidal gold are routinely used in histochemistry for the biospecific labelling of certain regions of tissue samples and subsequent TEM analysis. In contrast, applications of DNA-functionalised Au particles were introduced only a few years ago by Mirkin and co-workers.[58] The DNA-directed nanoparticle aggregates depicted in Figure 2 can be used for simple and cheap sensors in biomedical diagnostics, for example for the detection of nucleic acids from pathogenic organisms. Therefore, the major field of applications of AuNP 3D-assemblies concerns the diagnostics of nucleic acid. Many excellent review articles are available[9,16,17,59,60] summarising this field of application. However, most of the analytical

applications are based on solid-supports (see below), and therefore we will highlight just a few representative examples of 3D assembly in homogeneous solution here.

The sensitive detection of nucleic acids in homogeneous solutions has been achieved by self-assembled oligomerisation[61] or by the use of DNA beacons tethered to nanoparticles.[62] DNA beacons are single-stranded DNA (ssDNA) molecules that form an intramolecular hairpin-loop structure.[63] Both ends are chemically modified with a fluorophore and a quencher dye, the latter of which, due to close spatial proximity, effectively quenches the fluorescence. Upon hybridisation with nucleic acid targets containing a sequence stretch complementary to the loop region of the beacon, the quencher is spatially removed from the fluorophore, which leads to a strong enhancement in fluorescence. A novel class of molecular beacons has been introduced in which the organic quencher dye is replaced by a gold nanoparticle.[62] The quenching efficiency was determined to be about 99.5%, which indicates that the fluorescent signal of the beacon increases about 200-fold upon hybridisation with a complementary target. This type of gold-oligomer-dye hybrid beacon allows the detection of single-base mutations more efficiently than conventional molecular beacons.

Another very interesting observation has been reported by Maeda et al.,[64,65] who discovered that the aggregation of gold nanoparticles even occurs by non-cross-linking DNA hybridisation. This principle might be utilized to design novel assays for the rapid detection of nucleic acid targets.

The DNA-directed assembly of AuNPs has been coupled with functional DNA structures that are capable of carrying out a specific cleavage reaction. With respect to the enzyme-like performance, such a sequence is called a "DNAzyme". The incorporation of a DNAzyme into the particle-interconnecting DNA oligonucleotides allows the rapid and sensitive detection of a range of targets, such as Pb^{2+} ions or adenosine.[66–68]

In addition to the immediate applications of 3D-assembly in diagnostics, the DNA molecules attached to the nanoparticles can also be utilized as actuators for the assembly and switching of (bio)chemical reactions.[22] For instance, gold nanoparticle–DNA molecular beacon conjugates have been exploited for the remote electronic control of DNA hybridisation.[69] Inductive coupling of a radio-frequency magnetic field (RFMF) with a frequency of 1 GHz to the 1.4-nm metal nanoparticle, which functions as an antenna in the DNA constructs, leads to an increase in the local temperature of the bound DNA, thereby inducing denaturation while leaving surrounding molecules relatively unaffected. Since inductive heating has already been applied to the treatment of cancer cells with magnetic-field-induced excitation,[70] the use of gold nanocrystal–DNA conjugates should allow extension of this concept to novel applications. For instance, complex operations, such as gene regulation, biomolecular assembly and enzymatic activity, of distinct portions of nucleic acids or proteins might be controlled, while the rest of the molecule and neighbouring species would remain unaffected. Moreover, because the control is not optical, this technology could even be applicable in highly scattering media.[69]

Another example concerns the reversible switching of gold nanoparticle aggregation by means of "fuelling oligonucleotides" F_a and F_d in Figure 3.[23] The base sequence of F_a is comprised of three stretches, a′ and b′, which are complementary to 23-nm Au-nanoparticle-bound 12-mer oligomers a and b, respectively, as well as stretch c′, which promotes hybridisation of F_a and F_d. The transformation cycle starts with state I, in which the DNA–nanoparticles are dispersed and reveal a characteristic plasmon absorption maximum at 526 nm. Upon addition of oligomer F_a, the particles aggregate (state II in Figure 3), and consequently the plasmon absorption band is damped and shifted towards longer wavelengths at about 625 nm. In the next step, oligomer F_d is added, which is fully complementary to F_a and can hybridize with it, starting at the dangling end stretch c′ of the duplex DNA interconnecting the nanoparticles. This process, schematically shown as an intermediate state III in Figure 3, leads to the formation of a waste duplex and the redispersion of the nanoparticles. Hence, an increase in absorbance at 526 nm occurs again. Because this paper demonstrated for the first time that nanoparticle aggregation can be reversed at room temperature under physiological conditions, applications in the area of switchable (bio)materials for technical purposes and prosthetics might be foreseen.[23]

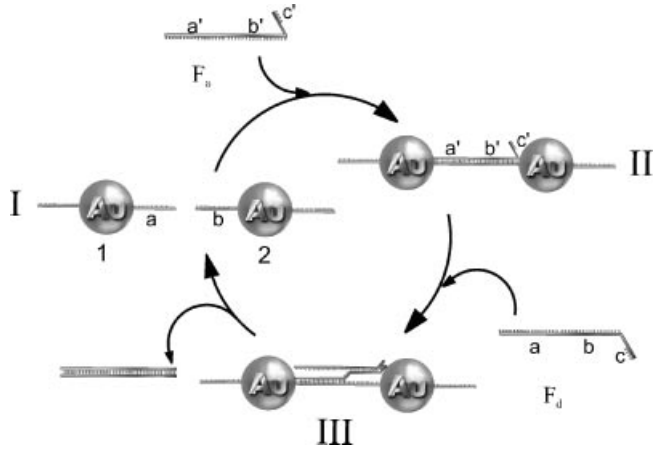

Figure 3. Schematic drawing of the reversible aggregation of DNA-modified gold nanoparticles utilizing fuelling oligonucleotides (F_a and F_d) containing three stretches (a, b and c) that are complementary to the gold-nanoparticle-bound 12-mer oligomers (a and b). Stretch c′ forms a dangling end in the aggregated particles (state II) which promotes the hybridisation of F_a and F_d (intermediate state III). Reprinted with permission, from ref.[23].

3.2. Two-Dimensional Assemblies

3.2.1. Assembly at Interfaces for Diagnostic Applications

In addition to the 3D assembly in homogeneous solution, the use of DNA-functionalised nanoparticles in the heterogeneous nucleic acid hybridisation with capture oligo-

nucleotides attached to solid supports has recently attracted much attention. Many groups have reported the DNA-directed immobilisation of gold nanoparticles to form supramolecular surface architectures,[71–80] and this approach has also been adopted to the specific sorting of DNA-functionalised quantum dots.[81] The specific nucleic acid-mediated immobilisation of gold nanoparticles can be utilized for the topographic labelling of surface-bound DNA targets. This readily allows the highly sensitive scanometric detection of nucleic acids in DNA-chip analyses by means of the gold-particle-promoted reduction of silver ions (Figure 4), which allows an almost 100-fold increase in sensitivity compared to conventional fluorescent DNA detection.[71] This approach has also been adopted for the array-based electronic detection of nucleic acid analytes.[79] To this end, DNA-functionalised nanoparticles have been immobilized in the gaps of microelectrodes by biospecific interaction. However, the particle density was too low to allow electron conduction between the electrodes. Thus, in a subsequent step, the nanoparticle assembly had to be metallized by reductive deposition of silver, which finally led to a conducting contact between the electrodes. The resulting decrease in ohmic resistance was used as a positive signal for the sensing of the biospecific interaction to be detected.[79]

The use of colloidal gold nanoparticles also allows signal enhancement in DNA hybridisation detection using a quartz crystal microbalance,[72,75] angle-dependent light scattering[82] and surface-plasmon resonance (SPR).[83]

The size-selective light scattering of 50- and 100-nm diameter Au nanoparticles has been used for the two-colour labelling of oligonucleotide arrays.[78] An alternative for the simultaneous determination of multiple DNA targets, the use of Raman-active dye labelled gold nanoparticles, has recently been explored.[84] The gold nanoparticles facilitate the formation of a silver coating that acts as a surface-enhanced Raman scattering promoter for the dye-labelled particles that have been captured by target molecules and an underlying chip in a microarray format. This approach provides the high sensitivity and high selectivity attributes of grey-scale scanometric detection but adds multiplexing and ratioing capabilities because a very large number of probes can be designed based on the concept of using a Raman tag as a narrow-band spectroscopic fingerprint.

DNA-tagged proteins have been immobilized at DNA-functionalised gold nanoparticles by specific nucleic acid hybridisation.[85] This approach has several advantages over the conventional methods to adsorb proteins to colloidal gold. The biofunctionalised nanoparticles not only retain

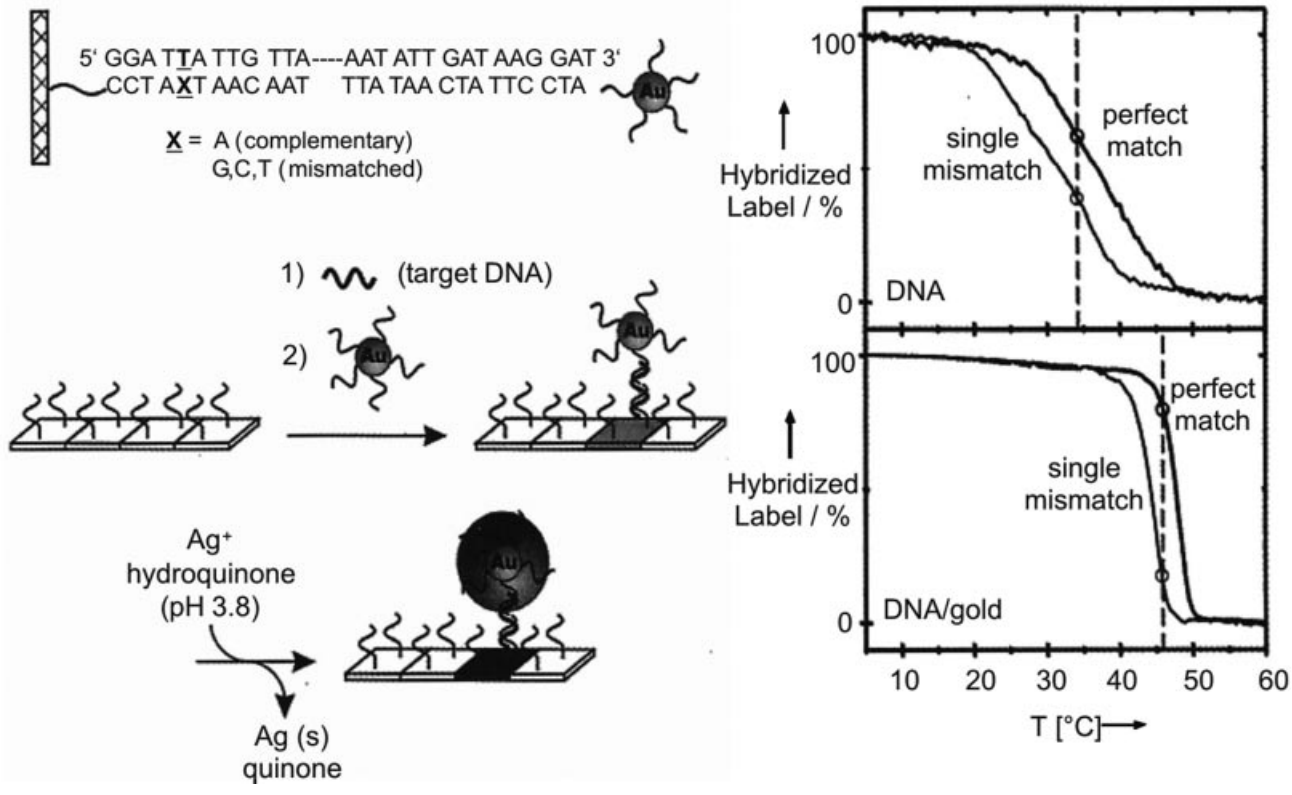

Figure 4. Scanometric detection of nucleic acids in DNA-chip analyses. Capture oligonucleotides immobilized on glass slides are used for specific binding of target nucleic acids. Oligonucleotide-functionalised gold nanoparticles are employed as probes in solid-phase DNA hybridisation detection. Subsequent to a silver enhancement step, the immobilisation of the colloidal gold probe is detected by scanning the glass substrate with a conventional flat-bed scanner. Despite its simplicity, this technique allows for an almost 100-fold increased sensitivity compared to fluorescent DNA detection. Moreover, due to the extraordinarily sharp melting behaviour of the immobilized DNA–nanoparticle networks (see melting curves on the right), this method allows for single-mismatch detection. Reprinted with permission from ref.[71], copyright 2000, American Association for the Advancement of Science.

the undisturbed recognition properties of the proteins immobilized, but they also reveal an extraordinary stability that even allows for regeneration of the DNA-coated gold particles. These type of bioinorganic hybrid components have been used as reagents in sandwich immunoassays for the detection of proteins using the gold-particle-promoted silver development, allowing for the spatially-addressable detection of femtomolar amounts of chip-immobilized antigens.[85] Recently, this approach was adopted to difunctional DNA AuNPs, thereby significantly enhancing the versatility of nanoparticle probes.[86] Moreover, DNA AuNPs with antibody molecules attached have been used as probes in the sensitive detection of proteins by means of the biobarcode approach.[87–90] These types of metal nanoparticle-based detection systems have been recently reviewed elsewhere.[10,91]

3.2.2. 2D-Assembly for Novel Materials

While monofunctional DNA–nanoparticle conjugates containing just a single recognition site, i.e. an oligonucleotide sequence, were employed in the studies described above, we have recently explored oligofunctional gold nanoparticle conjugates containing different DNA sequences (**D_n-Au** in Figure 1).[42] This type of particle can be considered as a "versatile particle", since, due to the extraordinary specificity of Watson–Crick base-pairing, the various oligonucleotide sequences can be individually and selectively addressed as members of an orthogonal coupling system present at the particle's surface.

As an example, we have shown that difunctional DNA–nanoparticle conjugates (**D_2-Au**) containing two different DNA oligomers self-assemble by DNA hybridisation into surface-bound layers comprised of closely packed, cross-linked nanoparticles (Figure 1).[92] In this approach, the two different DNA sequences of **D_2-Au_A** were utilized such that particle-bound oligomer **1** was used for immobilisation purposes by connecting the particles to surface-bound capture oligomers **4** through the complementary linker **5**. The second type of particle-bound oligomers (**2**) of **D_2-Au_A** was used to establish cross-links to neighbouring particles (**D_2-Au_B** in Figure 1) by means of linker **6**, which is complementary to the sequences **2** and **3** attached to particles **D_2-Au_A** and **D_2-Au_B**, respectively. We reasoned that this approach should lead to densely packed and potentially even ordered monolayers of nanoparticles in which the distance between the individual particles should be adjustable by changing the length of **6**.[92] While the initial study clearly proved the concept of inter-particle DNA cross-linking, no influence of **6** on the interparticle distances was observed by scanning force microscopy (SFM) analysis.[92]

In a recent continuation using in situ SFM studies, we have shown that the self-assembly of difunctional DNA-modified gold nanoparticles at solid substrates does indeed generate particle layers with programmable interparticle spacings.[93] A comparison of these results with earlier work[55,92] indicated that the DNA spacers are highly sensitive to environmental conditions, particularly the degree of hydration of the DNA double helix. Further exploration and refinement of this approach, especially the careful design of the oligomer sequences involved,[94] may eventually pave the way towards nanostructured materials with programmable functionalities for a broad range of applications in materials research and nanobiotechnology.[93]

3.3. One-Dimensional Assemblies

Two fundamentally different approaches have been applied for the formation of one-dimensional assemblies of metal nanoparticles along a DNA backbone. The first approach is to immobilize pre-formed nanoparticles preferably at specific sites along the DNA backbone, while the second approach applies to the direct metallisation of the DNA double strand by reducing the charge-compensation cations (e.g. Ag^+, Pd^{2+}) that were introduced by ion-exchange before. Both procedures have their inherent advantages and disadvantages. While the site-selective immobilisation of pre-formed nanoparticles can take advantage of the precise size control and the defined surface chemistry of the well-elaborated synthetic routes, it is a difficult task to assemble the particles in direct contact to each other over extended domains with an interparticle spacing that is identical and small enough to allow direct dipolar coupling or even electronic transport along the array. The metallisation by metal-ion reduction has successfully led to the formation of highly-conductive nanowires, which could be applied as metallic interconnects. However, the nanoparticles formed during this process suffer from an extraordinarily broad size distribution. Thus, the metal structures along the DNA wires are highly disordered, and none of the size-specific electronic transport properties, which are based on single-electron tunnelling, could be observed or even utilized in nanodevices. In the following section we give an overview of the different methods that have been developed following these two strategies by means of selected examples.

3.3.1. Immobilisation of Nanoparticles on DNA

As previously demonstrated for proteins,[95] Alivisatos and co-workers showed for the first time that a discrete number of water-soluble Au_{55} clusters with one *N*-propylmaleimide ligand per cluster can couple selectively to a sulforyl group incorporated into ssDNA oligomers.[96] Oligonucleotides modified at either the 3′- or 5′-terminus with a free sulforyl group were coupled with an excess of the nanoparticles. After being combined with suitable oligonucleotide templates, parallel (head-to-tail) and antiparallel dimers (head-to-head) were obtained (**7a**–**7c**, respectively, see part B in Figure 5). The linear alignment of the clusters and the centre-to-centre distance, which ranged from 2–6 nm, were illustrated by means of TEM images. These nanoparticle–DNA conjugates have a high flexibility when the DNA backbone is nicked, while an un-nicked double helix significantly lowers the flexibility (for instance, see **7d** in Figure 5). UV/Vis absorbance measurements indicated changes in the spectral properties of the nanoparticles as a consequence of the supramolecular organisation.[97]

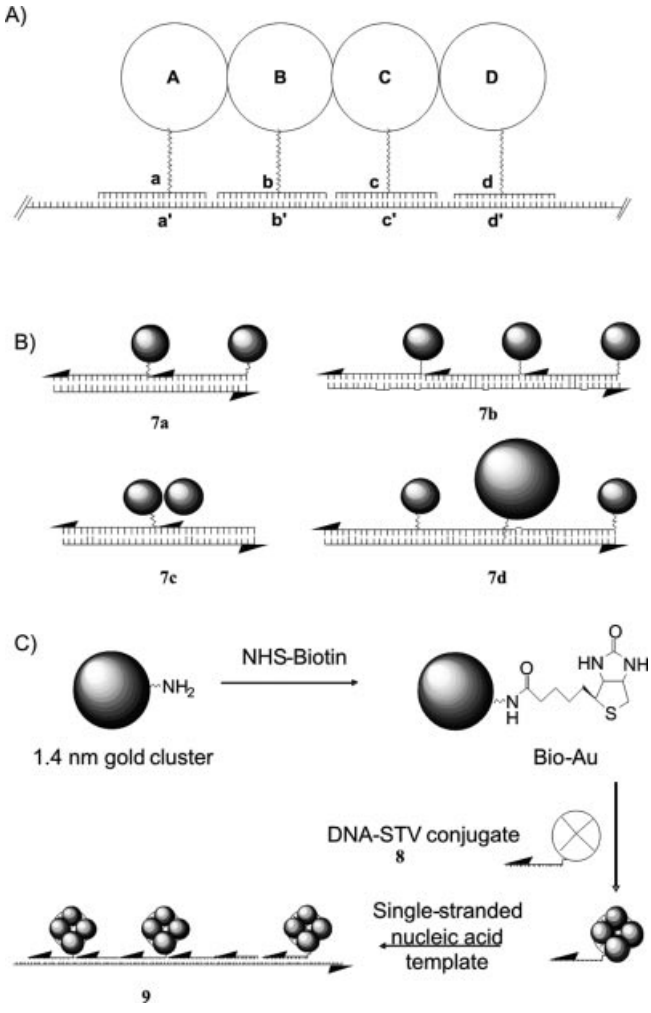

Figure 5. A) Schematic representation of DNA-directed one-dimensional assembly of four different nanoscale building blocks to form a stoichiometrically and spatially defined supramolecular aggregate. B) Assembly of nanocrystal molecules using DNA hybridisation. Conjugates from gold particles (represented as shaded spheres) and 3′- or 5′-thiolated oligonucleotides allow the fabrication of head-to-head (**7a**) or head-to-tail (**7b**) homodimers. A template containing the complementary sequence in triplicate effects the formation of the trimer **7c**. Aggregate **7d** has limited flexibility due to the un-nicked double helical backbone. C) DNA-directed assembly of biotinylated gold nanoclusters using covalent DNA-STV conjugates **8** as molecular adaptors. The nanocluster-loaded STV conjugates self-assemble in the presence of a single-stranded nucleic acid carrier molecule containing complementary sequence stretches to form biometallic aggregates, such as **9**. Reprinted with permission from C. M. Niemeyer, *Angew. Chem. Int. Ed.* **2001**, *40*, 4128–4158.

Noyong et al. have reported the synthesis of string-of-pearl-like alignments of 4-nm Au nanoparticles along DNA strands.[98] In the first step, *cis*-$[PtCl_2(NH_3)_2]$ (cisplatin) is incorporated into DNA-double strands of DNA plasmids. This platinum complex has a high affinity for nitrogen donor sites in nucleotides and therefore binds with high selectivity in neighbouring guanine-guanine nucleobases.[99] This process is well established in medicine, where cisplatin has been used as an anticancer drug for more than 30 years. In its intra-strand position Pt^{2+} is accessible for ligand exchange. Therefore, in a second step, the nanoparticles stabilized by cysteamine can selectively bind to the Pt^{2+} centre by exchange of the NH_3-ligands with H_2N-termini of the ligand shell (Figure 6).

The initial demonstration of the use of DNA as a framework for the precise spatial arrangement of molecular components was carried out with covalent conjugates of single-stranded DNA oligomers and the STV protein.[95] Using the STV-DNA conjugates **8** (Figure 5B) as model systems, a variety of essential basic studies on the DNA-directed assembly of macromolecules were carried out, which have been reviewed earlier.[100] The covalently attached oligonucleotide moiety supplements the STV's four native biotin-binding sites with a specific recognition domain for a complementary nucleic acid sequence. This biospecificity allows the use of DNA-STV conjugates as adapters to assemble basically any biotinylated compound along a nucleic acid template.[100] For example, the strong biotin-STV interaction and the specific nucleic acid hybridisation capabilities of the DNA-STV conjugates **8** have been utilized to organize gold nanoparticles (Figure 5C).[101] To this end, 1.4-nm gold particles containing a single amino substituent have been derivatized with a biotin group and the resulting biotin moiety subsequently used to organize the nanoparticles into a tetrahedral superstructure defined by the biotin-binding sites of the STV. Subsequently, the nanoparticle-loaded proteins self-assemble in the presence of a complementary single-stranded nucleic acid carrier molecule to form nanoparticle assemblies such as **9** (Figure 5C).

The strong biotin–STV interaction together with the specific nucleic acid hybridisation capabilities of DNA have recently been utilized for the controlled assembly of 5-nm Au particles along linear arrays of DNA triple cross-over molecules (TX).[102] As illustrated in Figure 7, the TX molecule consists of seven oligonucleotides, which are hybridized to form three double-stranded helices. These lie in a plane and are linked by strand exchange at four immobile crossover points. The design of the TX molecule is shown in part a of Figure 7. It contains two protruding stem loops, one each from the upper and the lower helices. Thus, a linear array of TX molecules can be obtained by designing three pairs of sticky ends. For illustration, their complementarity is represented by matching colour and geometric shape in part b of Figure 7. In order to template the assembly of 5-nm nanoparticles, streptavidin molecules were selectively bound to biotin groups, which are incorporated into the hairpin loops and are indicated by the small blue dots. In the next step, Au nanoparticles were conjugated to the streptavidin, resulting in a periodic sequence of uniform particles along the linear TX DNA. Figure 7 (parts c and d) shows SEM images of streptavidin/DNA-templated Au nanoparticle arrays. In the first template (c), only one stem loop in each TX molecule is modified with biotin groups, whereas in the second template (d) both stem loops are modified with biotin groups, leading to the formation of single and double rows of nanoparticles, respectively.[102] Kiehl and co-workers have reported similar approaches that use self-assembled DNA nanoarrays comprised of crossover

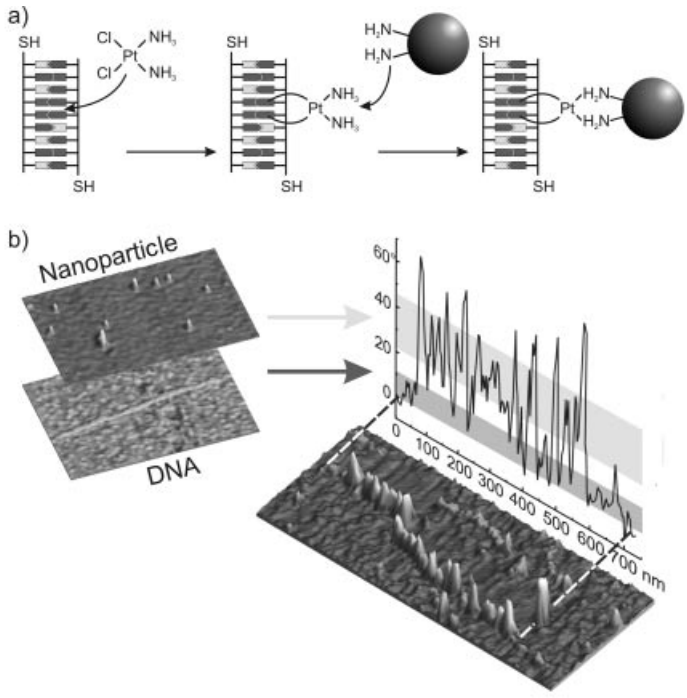

Figure 6. a) Scheme for the organisation of Au nanoparticles along DNA by coupling of NH_2-functionalised (cysteamine) Au nanoparticles at cisplatin-functionalised DNA by simple ligand replacement. b) AFM image (phase contrast) of DNA-aligned Au nanoparticles assembled on a silicon substrate (adapted from ref.[98]).

motifs to produce regular one- and two-dimensional assemblies of gold nanoparticles.[103,104] These reports suggest that programmable DNA arrays will open up novel, powerful routes to the production of precisely assembled nanoparticles.

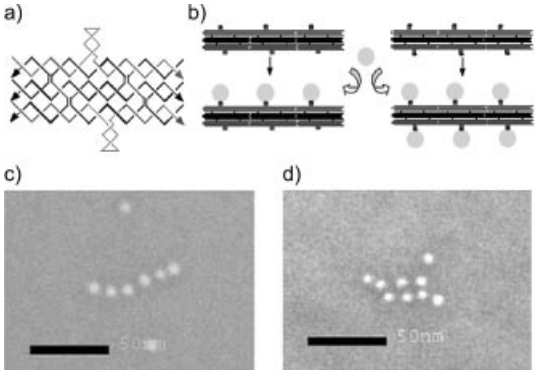

Figure 7. a) Design of the TX molecule and b) schematic drawing of the TX DNA-templated self-assembly of streptavidin linear arrays. c) and d) SEM images of the DNA-templated assembly of 5-nm Au particles (reproduced with permission from ref.[102]).

A first step towards device fabrication has been demonstrated by Kretschmer and Fritsche,[105] who have reported the integration of DNA-templated Au nanoparticles into microelectrode gaps. The microelectrode structures were fabricated by standard photolithography, and the assembly of nanowires consisting of Au nanoparticles in a string-of-pearl-like arrangement spanning the gap was achieved by dielectrophoresis. In a comprehensive study, the different control parameters of formation, the electrical transport properties and the stability of these arrays that lead finally to nanowires consisting of almost uniform nanoparticles that exhibit ohmic behaviour were analysed. The most important results of that work are displayed in Figure 8, which shows SEM images of nanowires bridging an electrode gap of 1 μm. Dielectrophoresis leads to a high number of nanowires, although the magnification shows that the main parts of these wires consist of pearl chains, whereas the diameter of the particles is about 15 nm. The zoom (inset in b) shows the excellent preservation of the individual particles.

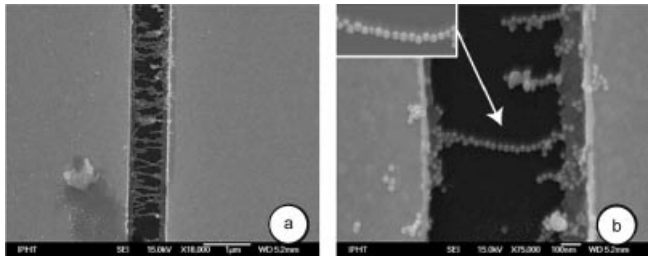

Figure 8. SEM images of microelectrode structure with immobilized DNA-templated nanowires (for explanation see text; reproduced with permission from ref.[105]).

By going to significantly smaller particles of 1.5 nm, which have a much greater potential to serve as building blocks in future nanoelectronic devices due to their enhanced charging energy, Hutchinson and co-workers have elaborated a method to organize the 1.5-nm gold particles

into linear chains with precisely controlled interparticle spacing over a range of 1.5–2.8 nm.[106,107] These chains are formed in solution by utilizing functional-group-directed self-assembly to organize ligand-stabilized gold nanoparticles onto DNA templates. In this configuration, the spacing between neighbouring nanoparticles is determined by the thickness of the ligand shell stabilizing the nanoparticles and can therefore be tuned at the molecular level by variation of the ligand shell at spacings of 1.5, 2.1 and 2.8 nm with a standard deviation of ≤20%. The ligands that are used for this immobilisation process are (2-mercaptoethyl) trimethylammonium iodide (TMAT, **1**), [2-(2-mercaptoethoxy)ethyl]trimethylammonium toluene-4-sulfonate (MEMA, **6**), and {2-[2-(2-mercaptoethoxy)ethoxy] ethyl}trimethylammonium toluene-4-sulfonate (PEGNME, **11**).

Because the interparticle spacing is enforced by the ligand shell rather than by the scaffold, the spacing is uniform even in nonlinear sections of the chain. This allows the assembly of particles over extended areas up to 1 μm in length and a total coverage of >90%. Figure 9 shows the immobilisation scheme and representative TEM images of linear nanoparticle chains of Au_n-TMAT, Au_n-MEMA and Au_n-PEGNME assembled on λ-DNA. The spacing between neighbouring nanoparticles increases systematically with increasing ligand shell thickness from 1.5 nm ± 0.3 nm in Figure 9A (Au_n-TMAT), through 2.1 ± 0.4 nm in Figure 9B (Au_n-MEMA) to 2.8 nm ± 0.4 nm in Figure 9C (Au_n-PEGNME). The interparticle spacing corresponds to the double thickness of the ligand shell assuming that the stabilizing ligands are in a fully extended conformation, i.e. 1.4 nm for TMAT-functionalised nanoparticles, 2.1 nm for nanoparticles stabilized by MEMA and 2.8 nm for PEGNME-functionalised nanoparticles. The small standard deviations indicate the reproducibility and reliability of this method for generating evenly spaced nanoparticle chains with a high degree of control.

Besides DNA, other chain-like bimolecules have also been used for the one-dimensional assembly. As an example, Bae et al. have recently demonstrated the assembly of one-dimensional arrays of 5-nm Au-nanoparticles using schizophyllan (SPG).[108] SPG is a natural polysaccharide produced by the fungus *Schyzophyllum commune*, which adopts a triple-helical conformation under native conditions. This structure was reversibly dissociated into single chains, which then served as the template for the assembly of the nanoparticles during triple-helix formation.

3.3.2. Metallisation of DNA

Direct metallisation of DNA has been employed by Braun et al. in order to create conductive silver wires.[109] In a multistep process, lithographically fabricated gold elec-

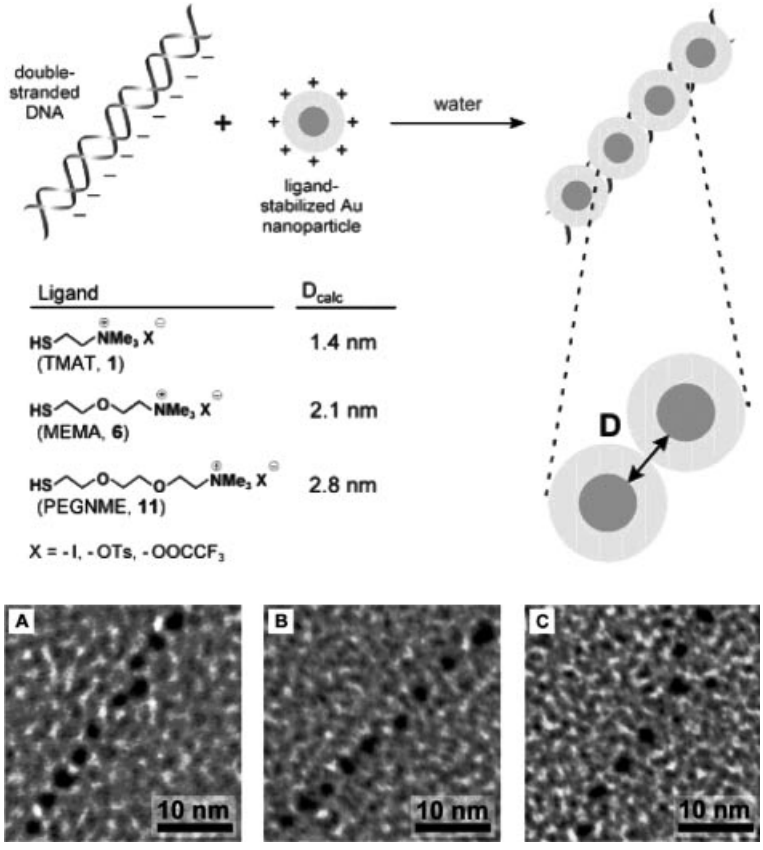

Figure 9. Schematic representation of the solution-phase formation of linear, close-packed DNA–nanoparticle assemblies. The three ligands used are shown in the figure. Below: the TEM images of linear, close-packed nanoparticle–DNA assemblies. The TEM micrographs demonstrate the use of three different ligands to produce linear arrays with different spacing between neighbouring nanoparticles (reproduced with kind permission from ref.[106]).

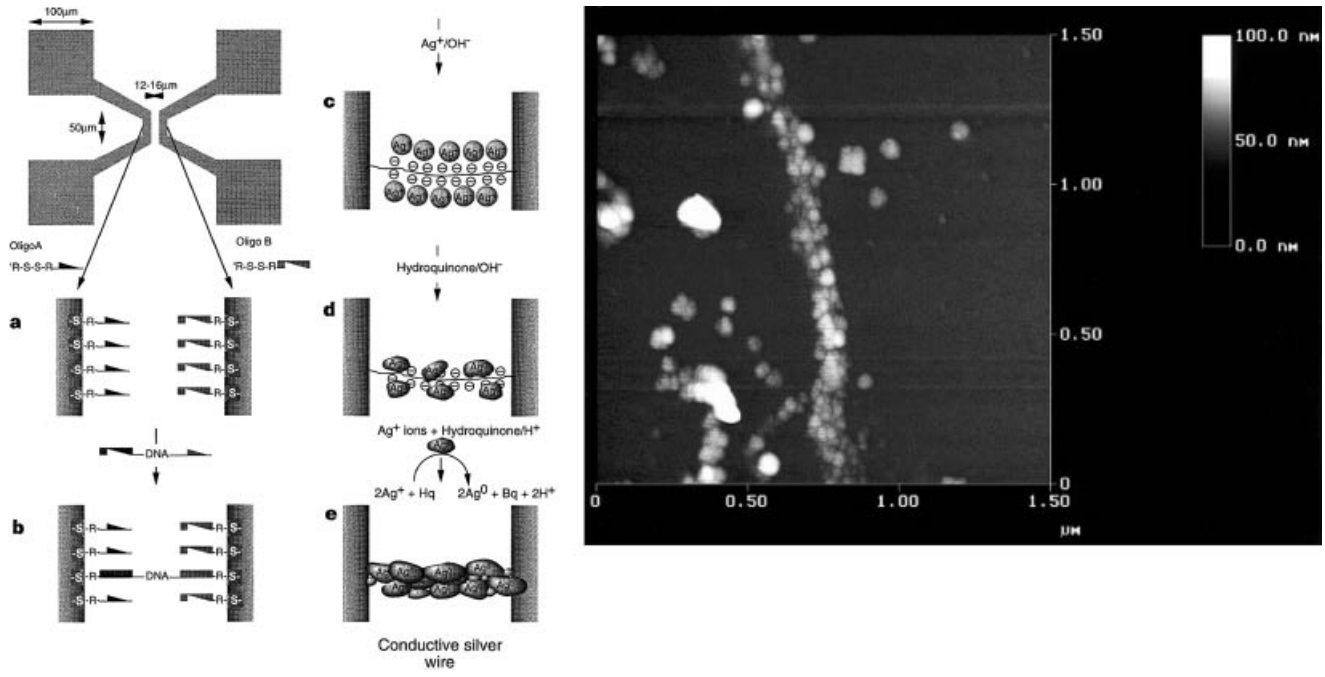

Figure 10. Left: Construction of a nanowire bridging the gap between two gold electrodes. The Ag^+ ions were deposited on the DNA bridge and subsequently reduced to form metallic nanoparticle agglomerates. Right: AFM image of the nanowires illustrating the granular structure (reproduced with permission from ref.[109]).

trodes were functionalised with disulfide-functionalised 12-base oligonucleotides. DNA that contains two 12-base sticky ends, where each of the ends is complementary to one of the two different sequences, was attached to the gold electrodes. Then, an Ag^+ solution was introduced to the surface, which induced an exchange of the charge-compensating Na^+ ions by Ag^+. Reduction with hydroquinone induced the formation of DNA-associated Ag^0 aggregates along the DNA strand. In a following development process, further Ag^+ was reduced to finally provide the metal growths, leading to individual silver nanowires with an average diameter of 100 nm with a pronounced granular structure.

The AFM image in Figure 10 indicates that the wire consists of grains 30–50 nm in diameter deposited along the DNA skeleton. Two-terminal electrical measurements on the silver wire showed that, depending on the silver growth conditions, the differential resistance at voltages beyond the plateau, which is caused presumably by Coulomb charging and/or corrosion effects, varies between 7 and 30 MΩ. Recent continuation of this work has demonstrated original and innovative concepts for tailoring the structural diversity and connectivity of DNA architectures, which is essential for the construction of more complex electronic components and circuits.[110,111]

A similar procedure has also been applied by Harnack et al.[112] and by Richter et al.[113] Harnack et al. have immobilized tris(hydroxymethyl)phosphane-capped gold nanoparticles 1–2 nm in diameter densely on calf thymus DNA. These particles are active catalysts for electroless plating of gold leading to the formation of nanowires with widths of 30–40 nm and electrical conductivities about one-thousandth that of bulk gold. Richter et al. metallized λ-DNA with palladium. The metallisation was accomplished in a two-step chemical deposition of the metal, involving binding of $Pd(CH_3COO)_2$ to the DNA and subsequent reduction with sodium citrate, lactic acid or dimethylborane. This reduction led to the formation of chains of Pd nanoparticles along the DNA (Figure 11). These wires were found to be conducting, exhibiting ohmic behaviour at room temperature. The authors developed this method further by using K_2PtCl_4 and K_2PdCl_4 as a metal source and by slight modification of the reducing conditions.[114] This led to the formation of ordered chains of nanoparticles, thus illustrating a remarkable control over the nucleation and growth processes.

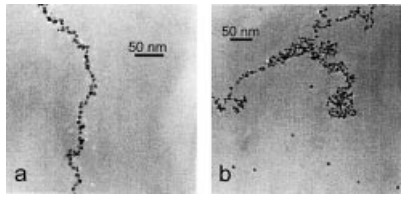

Figure 11. TEM micrographs of chains of a) Pt and b) Pd clusters grown on λ-DNA (reproduced with permission from ref.[114]).

4. Conclusions and Future Directions

This article is intended to provide an overview of the current state-of-the-art of DNA-based assembly of metal nanoparticles in one, two and three dimensions. The examples selected show that interdisciplinary research at the frontier between biomolecular chemistry, inorganic chemis-

try and materials science leads to new materials with unique properties.

While the assembly process itself is based on the enormous specificity of nucleic acids, which can be tailored by virtue of synthetic organic chemistry, much remains to be done in the development of the basic building blocks, i.e. the DNA AuNPs. As such, there is still a tremendous demand for alternative methods to allow for compensation of typical problems arising in the biofunctionalisation of inorganic nanoparticles. In particular, harsh assembly conditions may lead to ligand-exchange reactions occurring at the colloidal surface. This often prevents the formation of stable bioconjugates and efficient supramolecular assembly. Moreover, the synthesis of nanoparticle–nucleic acid conjugates that are well-defined with respect to their stoichiometric composition is a great challenge, and it is particularly important, from a molecular engineering point of view, to generate sophisticated nanoarchitectures.

Another very important goal concerns the de novo design of nucleic acid sequences that allow efficient two- and three-dimensional self-assembly. Bioinformatic approaches appear to be well suited for solving this task,[94] although much remains to be done in the refinement of such tools. Once developed, one may anticipate a broad scope of applications for designing nucleic acid scaffolds to be used for both the assembly of surface-bound nanoparticle architectures as well as three-dimensional aggregates for bioanalytical and advanced materials research.

When DNA is used as a template for the assembly of nanoparticles, the examples given in this review show impressively that nanowires with metallic conductivity can be obtained. These results have already prompted exciting research on the set-up of functional devices of higher complexity. The works of Williams et al.,[115] who has utilized the recognition of DNA to bind carbon nanotubes to metallic contacts by self-assembly, and by Keren et al.,[110] who has described the self-assembly of segmented nanowires in a multi-step self-assembly process, are emphasised as promising examples. However, it is still a great challenge to develop these processes further in order to realize devices or even device architectures that are robust enough to be applied in nanoelectronic circuitry.

Acknowledgments

Our work is supported by Deutsche Forschungsgemeinschaft (DFG) in Schwerpunktprogramm 1072 through grants Ni399/4-1-3 (CMN), Si609/3-1 and 4-1,2 (US). We thank Bülent Ceyhan and Michael Noyong for help with the figures.

[1] M. Faraday, *Philos. Trans. R. Soc.* **1857**, *147*, 145.
[2] J. M. Thomas, *Pure Appl. Chem.* **1988**, *60*, 1517.
[3] U. Kreibig, M. Vollmer, *Optical Properties of Metal Clusters*, Springer, New York, **1995**.
[4] G. Schoen, U. Simon, *Colloid Polymer Sci.* **1995**, *273*, 101–117.
[5] D. L. Feldheim, C. A. Foss, *Metal Nanoparticles: Synthesis Characterisation, and Applications*, Marcel Dekker, New York, **2002**.
[6] U. Simon, *Adv. Mater.* **1998**, *10*, 1487–1492.
[7] G. Schmid, *Nanoparticles: From Theory to Application*, Wiley-VCH, Weinheim, **2004**.
[8] L. J. De Jongh, *Physics and Chemistry of Metal Cluster Compounds* **1994**.
[9] E. Katz, I. Willner, *Angew. Chem. Int. Ed.* **2004**, *43*, 6042–6108.
[10] N. L. Rosi, C. A. Mirkin, *Chem. Rev.* **2005**, *105*, 1547–1562.
[11] F. Remacle, R. D. Levine, *ChemPhysChem.* **2001**, *2*, 21–36.
[12] G. Markovich, C. P. Collier, J. R. Heath, *Phys. Rev. Lett.* **1998**, *80*, 3807–3810.
[13] G. Schmid, M. Baumle, N. Beyer, *Angew. Chem. Int. Ed.* **2000**, *39*, 181–183; *Angew. Chem.* **2000**, *112*, 187.
[14] G. Schmid, U. Simon, *Chem. Commun.* **2005**, 697–710.
[15] S. Liu, R. Maoz, G. Schmid, J. Sagiv, *Nano Lett.* **2002**, *2*, 1055–1060.
[16] C. A. Mirkin, *Inorg. Chem.* **2000**, *39*, 2258–2272.
[17] C. M. Niemeyer, *Angew. Chem. Int. Ed.* **2001**, *40*, 4128–4158; *Angew. Chem.* **2001**, *113*, 4254–4287.
[18] C. M. Niemeyer, *Angew. Chem. Int. Ed.* **2003**, *42*, 5796–5800; *Angew. Chem.* **2003**, *115*, 5974–5978.
[19] M. H. Caruthers, *Science* **1985**, *230*, 281–285.
[20] K. B. Mullis, *Angew. Chem. Int. Ed. Engl.* **1994**, *33*, 1209–1213; *Angew. Chem.* **1994**, *106*, 1271–1276.
[21] N. C. Seeman, *Nature* **2003**, *421*, 427–431.
[22] C. M. Niemeyer, M. Adler, *Angew. Chem. Int. Ed.* **2002**, *41*, 3779–3783; *Angew. Chem.* **2002**, *114*, 3933–3937.
[23] P. Hazarika, B. Ceyhan, C. M. Niemeyer, *Angew. Chem. Int. Ed.* **2004**, *43*, 6469–6471; *Angew. Chem.* **2004**, *116*, 6631–6633.
[24] R. M. Stoltenberg, A. T. Woolley, *Biomed Microdevices* **2004**, *6*, 105–111.
[25] B. G. Ershov, E. Janata, M. Michaelis, A. Henglein, *J. Phys. Chem.* **1991**, *95*, 8996–8999.
[26] A. Henglein, M. Gutierrez, E. Janata, B. G. Ershov, *J. Phys. Chem.* **1992**, *96*, 4598–4602.
[27] J. R. Thomas, *J. Appl. Phys.* **1966**, *37*, 2914–2915.
[28] W. Yu, W. Tu, H. Liu, *Langmuir* **1999**, *15*, 6–9.
[29] N. A. Dhas, A. Gedanken, *J. Mater. Chem.* **1998**, *8*, 445–450.
[30] M. C. Daniel, D. Astruc, *Chem. Rev.* **2004**, *104*, 293–346.
[31] R. Richards, H. Boennemann, J. Hormes, C. Leuschner, in *Nanofabrication Towards Biomedical Applications* (Eds.: C. S. S. R. Kumar, J. Hormes), Wiley-VCH, Weinheim, **2005**, pp. 3–32.
[32] G. Schmid, R. Boese, R. Pfeil, F. Bandermann, S. Meyer, G. H. M. Calis, J. W. A. van der Velden, *Chem. Ber.* **1981**, *114*, 3634.
[33] G. Schmid, B. Morun, J.-O. Malm, *Angew. Chem. Int. Ed. Engl.* **1989**, *28*, 778–780.
[34] M. N. Vargaftik, V. P. Zagorodnikov, I. P. Stolyarov, I. I. Moiseev, V. A. Likholobov, D. I. Kochubey, A. L. Chuvilin, V. I. Zaikovsky, K. I. Zamaraev, G. I. Timofeeva, *J. Chem. Soc., Chem. Commun.* **1985**, 937–939.
[35] I. I. Moiseev, M. N. Vargaftik, T. V. Chernysheva, T. A. Stromnova, A. E. Gekhman, G. A. Tsirkov, A. M. Makhlina, *J. Mol. Catal. A* **1996**, *108*, 77–85.
[36] J. P. Spatz, A. Roescher, S. Sheiko, G. Krausch, M. Moeller, *Adv. Mater.* **1995**, *7*, 731–735.
[37] J. P. Spatz, A. Roescher, M. Moeller, *Adv. Mater.* **1996**, *8*, 337–340.
[38] M. T. Reetz, W. Helbig, *J. Am. Chem. Soc.* **1994**, *116*, 7401–7402.
[39] C. A. Mirkin, R. L. Letsinger, R. C. Mucic, J. J. Storhoff, *Nature* **1996**, *382*, 607–609.
[40] J. J. Storhoff, R. Elghanian, R. C. Mucic, C. A. Mirkin, R. L. Letsinger, *J. Am. Chem. Soc.* **1998**, *120*, 1959–1964.
[41] P. Hazarika, T. Giorgi, M. Reibner, B. Ceyhan, C. M. Niemeyer, in *Bioconjugation Protocols: Strategies and* Methods (Ed.: C. M. Niemeyer), Humana Press, Totowa, NJ, **2004**, in press.
[42] C. M. Niemeyer, B. Ceyhan, P. Hazarika, *Angew. Chem. Int. Ed.* **2003**, *42*, 5766–5770; *Angew. Chem.* **2003**, *115*, 5944–5948.

[43] L. M. Demers, C. A. Mirkin, R. C. Mucic, R. A. Reynolds, R. L. Letsinger, R. Elghanian, G. Viswanadham, *Anal. Chem.* **2000**, *72*, 5535–5541.
[44] D. Zanchet, C. M. Micheel, W. J. Parak, D. Gerion, A. P. Alivisatos, *Nano Lett.* **2001**, *1*, 32–35.
[45] W. J. Parak, T. Pellegrino, C. M. Micheel, D. Gerion, S. C. Williams, A. P. Alivisatos, *Nano Lett.* **2003**, *3*, 33–36.
[46] Y. Chen, J. Aveyard, R. Wilson, *Chem. Commun.* **2004**, 2804–2805.
[47] R. L. Letsinger, R. Elghanian, G. Viswanadham, C. A. Mirkin, *Bioconjugate Chem.* **2000**, *11*, 289–291.
[48] Z. Li, R. Jin, C. A. Mirkin, R. L. Letsinger, *Nucleic Acids Res.* **2002**, *30*, 1558–1562.
[49] R. Levy, N. T. Thanh, R. C. Doty, I. Hussain, R. J. Nichols, D. J. Schiffrin, M. Brust, D. G. Fernig, *J. Am. Chem. Soc.* **2004**, *126*, 10076–10084.
[50] G. P. Mitchell, C. A. Mirkin, R. L. Letsinger, *J. Am. Chem. Soc.* **1999**, *121*, 8122–8123.
[51] S.-J. Park, A. A. Lazarides, C. A. Mirkin, R. L. Letsinger, *Angew. Chem. Int. Ed.* **2001**, *40*, 2909–2912; *Angew. Chem.* **2001**, *113*, 2993–2996.
[52] J. K. N. Mbindyo, B. D. Reiss, B. R. Martin, C. D. Keating, M. J. Natan, T. E. Mallouk, *Adv. Mater.* **2001**, *13*, 249–254.
[53] E. Dujardin, L. B. Hsin, C. R. C. Wang, S. Mann, *Chem. Commun.* **2001**, 1264–1265.
[54] J. J. Storhoff, A. A. Lazarides, R. C. Mucic, C. A. Mirkin, R. L. Letsinger, G. C. Schatz, *J. Am. Chem. Soc.* **2000**, *122*, 4640–4650.
[55] S.-J. Park, A. A. Lazarides, C. A. Mirkin, P. W. Brazis, C. R. Kannewurf, R. L. Letsinger, *Angew. Chem. Int. Ed.* **2000**, *39*, 3845–3848; *Angew. Chem.* **2000**, *112*, 4003–4006.
[56] R. Jin, G. Wu, Z. Li, C. A. Mirkin, G. C. Schatz, *J. Am. Chem. Soc.* **2003**, *125*, 1643–1654.
[57] J. Kreuter, in *Microcapsules and Nanoparticles in Medicine and Pharmacy* (Ed.: M. Donbrow), CRC Press, Boca Raton, FL, **1992**, p. 125–148.
[58] J. J. Storhoff, C. A. Mirkin, *Chem. Rev.* **1999**, *99*, 1849–1862.
[59] A. N. Shipway, E. Katz, I. Willner, *ChemPhysChem.* **2000**, *1*, 19–52.
[60] C. M. Niemeyer, C. A. Mirkin (Eds.), *NanoBiotechnology: Concepts, Methods and Applications*, Wiley-VCH, Weinheim, **2004**.
[61] R. Elghanian, J. J. Storhoff, R. C. Mucic, R. L. Letsinger, C. A. Mirkin, *Science* **1997**, *277*, 1078–1081.
[62] B. Dubertret, M. Calame, A. J. Libchaber, *Nat. Biotechnol.* **2001**, *19*, 365–370.
[63] S. Tyagi, F. R. Kramer, *Nat. Biotechnol.* **1996**, *14*, 303–308.
[64] K. Sato, K. Hosokawa, M. Maeda, *J. Am. Chem. Soc.* **2003**, *125*, 8102–8103.
[65] K. Sato, M. Sawayanagi, K. Hosokawa, M. Maeda, *Anal. Sci.* **2004**, *20*, 893–894.
[66] J. Liu, Y. Lu, *J. Am. Chem. Soc.* **2004**, *126*, 12298–12305.
[67] J. Liu, Y. Lu, *Anal. Chem.* **2004**, *76*, 1627–1632.
[68] J. Liu, Y. Lu, *J. Fluoresc.* **2004**, *14*, 343–354.
[69] K. Hamad-Schifferli, J. J. Schwartz, A. T. Santos, S. Zhang, J. M. Jacobson, *Nature* **2002**, *415*, 152–155.
[70] A. Jordan, R. Scholz, P. Wust, H. Fähling, *J. Magn. Magn. Mater.* **1999**, *201*, 413–419.
[71] T. A. Taton, C. A. Mirkin, R. L. Letsinger, *Science* **2000**, *289*, 1757–1760.
[72] L. Lin, H. Zhao, J. Li, J. Tang, M. Duan, L. Jiang, *Biochem. Biophys. Res. Commun.* **2000**, *274*, 817–820.
[73] S. Han, J. Lin, F. Zhou, R. L. Vellanoweth, *Biochem. Biophys. Res. Commun.* **2000**, *279*, 265–269.
[74] R. Möller, A. Csaki, J. M. Köhler, W. Fritzsche, *Nucleic Acids Res.* **2000**, *28*, E91.
[75] F. Patolsky, K. T. Ranjit, A. Lichtenstein, I. Willner, *Chem. Commun.* **2000**, 1025–1026.
[76] T. A. Taton, R. C. Mucic, C. A. Mirkin, R. L. Letsinger, *J. Am. Chem. Soc.* **2000**, *122*, 6305–6306.
[77] C. M. Niemeyer, B. Ceyhan, S. Gao, L. F. Chi, S. Peschel, U. Simon, *Colloid Polym. Sci.* **2001**, *279*, 68–72.
[78] T. A. Taton, G. Lu, C. A. Mirkin, *J. Am. Chem. Soc.* **2001**, *123*, 5164–5165.
[79] S. J. Park, T. A. Taton, C. A. Mirkin, *Science* **2002**, *295*, 1503–1506.
[80] S. Peschel, B. Ceyhan, C. M. Niemeyer, S. Gao, L. F. Chi, U. Simon, *Mater. Sci. Eng., C* **2002**, *19*, 47–50.
[81] D. Gerion, W. J. Parak, S. C. Williamson, D. Zanchet, C. M. Micheel, A. P. Alivisatos, *J. Am. Chem. Soc.* **2002**, *124*, 7070–7074.
[82] G. R. Souza, J. H. Miller, *J. Am. Chem. Soc.* **2001**, *123*, 6734–6735.
[83] L. He, M. D. Musick, S. R. Nicewarner, F. G. Salinas, S. J. Benkovic, M. J. Natan, C. D. Keating, *J. Am. Chem. Soc.* **2000**, *122*, 9071–9077.
[84] Y. C. Cao, R. Jin, C. A. Mirkin, *Science* **2002**, *297*, 1536–1540.
[85] C. M. Niemeyer, B. Ceyhan, *Angew. Chem. Int. Ed.* **2001**, *40*, 3685–3688; *Angew. Chem.* **2001**, *113*, 3798–3801.
[86] P. Hazarika, B. Ceyhan, C. M. Niemeyer, *Small* **2005**, *1*, in press.
[87] J. M. Nam, S. I. Stoeva, C. A. Mirkin, *J. Am. Chem. Soc.* **2004**, *126*, 5932–5933.
[88] J. M. Nam, C. S. Thaxton, C. A. Mirkin, *Science* **2003**, *301*, 1884–1886.
[89] J. M. Nam, S. J. Park, C. A. Mirkin, *J. Am. Chem. Soc.* **2002**, *124*, 3820–3821.
[90] D. G. Georganopoulou, L. Chang, J. M. Nam, C. S. Thaxton, E. J. Mufson, W. L. Klein, C. A. Mirkin, *Proc. Natl. Acad. Sci. USA* **2005**, *102*, 2273–2276.
[91] C. M. Niemeyer, M. Adler, R. Wacker, *Trends Biotechnol.* **2005**, *23*, 208–216.
[92] C. M. Niemeyer, B. Ceyhan, M. Noyong, U. Simon, *Biochem. Biophys. Res. Commun.* **2003**, *311*, 995–999.
[93] B. Zou, B. Ceyhan, U. Simon, C. M. Niemeyer, *Adv. Mater.* **2005**, *17*, 1643–1647.
[94] U. Feldkamp, R. Wacker, W. Banzhaf, C. M. Niemeyer, *ChemPhysChem.* **2004**, *5*, 367–372.
[95] C. M. Niemeyer, T. Sano, C. L. Smith, C. R. Cantor, *Nucl. Acids Res.* **1994**, *22*, 5530–5539.
[96] A. P. Alivisatos, K. P. Johnsson, X. Peng, T. E. Wilson, C. J. Loweth, M. P. Bruchez Jr., P. G. Schultz, *Nature* **1996**, *382*, 609–611.
[97] C. J. Loweth, W. B. Caldwell, X. Peng, A. P. Alivisatos, P. G. Schultz, *Angew. Chem. Int. Ed.* **1999**, *38*, 1808–1812; *Angew. Chem.* **1999**, *111*, 1925–1929.
[98] M. Noyong, K. Gloddek, U. Simon, *Mater. Res. Soc. Symp. Proc.* **2003**, 153–158.
[99] E. R. Jamieson, S. J. Lippard, *Chem. Rev.* **1999**, *99*, 2467–2498.
[100] C. M. Niemeyer, *Chem. Eur. J.* **2001**, *7*, 3188–3195.
[101] C. M. Niemeyer, W. Bürger, J. Peplies, *Angew. Chem. Int. Ed.* **1998**, *37*, 2265–2268; *Angew. Chemie* **1998**, *110*, 2391–2395.
[102] H. Li, S. H. Park, J. H. Reif, T. H. LaBean, H. Yan, *J. Am. Chem. Soc.* **2004**, *126*, 418–419.
[103] S. Xiao, F. Liu, A. E. Rosen, J. F. Hainfeld, N. C. Seeman, K. Musier-Forsyth, R. A. Kiehl, *J. Nanoparticle Res.* **2002**, *4*, 313–317.
[104] J. D. Le, Y. Pinto, N. C. Seeman, K. Musier-Forsyth, T. A. Taton, R. A. Kiehl, *NanoLett.* **2004**, 2343–2347.
[105] R. Kretschmer, W. Fritzsche, *Langmuir* **2004**, *20*, 11797–11801.
[106] G. H. Woehrle, M. G. Warner, J. E. Hutchison, *Langmuir* **2004**, *20*, 5982–5988.
[107] M. G. Warner, J. E. Hutchison, *Nat. Mater.* **2003**, *2*, 272–277.
[108] A.-H. Bae, M. Numata, T. Hasegawa, C. Li, K. Kaneko, K. Sakurai, S. Shinkai, *Angew. Chem. Int. Ed.* **2005**, *44*, 2030–2033; *Angew. Chem.* **2005**, *117*, 2066–2069.
[109] E. Braun, Y. Eichen, U. Sivan, G. Ben-Yoseph, *Nature* **1998**, *391*, 775–778.

[110] K. Keren, M. Krueger, R. Gilad, G. Ben-Yoseph, U. Sivan, E. Braun, *Science* **2002**, *297*, 72–75.
[111] K. Keren, R. S. Berman, E. Buchstab, U. Sivan, E. Braun, *Science* **2003**, *302*, 1380–1382.
[112] O. Harnack, W. E. Ford, A. Yasuda, J. M. Wessels, *Nano Lett.* **2002**, *2*, 919–923.
[113] J. Richter, M. Mertig, W. Pompe, I. Monch, H. K. Schackert, *Appl. Phys. Lett.* **2001**, *78*, 536–538.
[114] R. Seidel, L. C. Ciacchi, M. Weigel, W. Pompe, M. Mertig, *J. Phys. Chem. B* **2004**, *108*, 10801–10811.
[115] K. A. Williams, P. T. Veenhuizen, B. G. de la Torre, R. Eritja, C. Dekker, *Nature* **2002**, *420*, 761.

Received: May 10, 2005
Published Online: August 26, 2005

